REPORT DOCUMENTATION PAGE

Form Approved OMB NO. 0704-0188

1. REPORT DATE (DD-MM-YYYY)	2. REPORT TYPE	3. DATES COVERED (From - To)
07-05-2016	Final Report	1-Apr-2015 - 31-Dec-2015

4. TITLE AND SUBTITLE
Final Report: Dielectric Sensing of Toxic and Explosive Chemicals via Impedance Spectroscopy and Plasmonic Resonance (research area 11: STIR)

5a. CONTRACT NUMBER
W911NF-15-1-0104

5b. GRANT NUMBER

5c. PROGRAM ELEMENT NUMBER

6. AUTHORS
Dr. S. James Allen, Dr. Adam J. Hauser

5d. PROJECT NUMBER

5e. TASK NUMBER

5f. WORK UNIT NUMBER

7. PERFORMING ORGANIZATION NAMES AND ADDRESSES
University of California - Santa Barbara
3227 Cheadle Hall
3rd floor, MC 2050
Santa Barbara, CA 93106 -2050

8. PERFORMING ORGANIZATION REPORT NUMBER

9. SPONSORING/MONITORING AGENCY NAME(S) AND ADDRESS (ES)
U.S. Army Research Office
P.O. Box 12211
Research Triangle Park, NC 27709-2211

10. SPONSOR/MONITOR'S ACRONYM(S)
ARO

11. SPONSOR/MONITOR'S REPORT NUMBER(S)
67105-CH-II.3

12. DISTRIBUTION AVAILIBILITY STATEMENT
Approved for Public Release; Distribution Unlimited

13. SUPPLEMENTARY NOTES
The views, opinions and/or findings contained in this report are those of the author(s) and should not contrued as an official Department of the Army position, policy or decision, unless so designated by other documentation.

14. ABSTRACT
The primary focus of this nine-month effort was to develop electronic sensors for hazardous chemicals. The first step was to identify material(s) that have interaction potential with chemicals of interest. In particular, specific reaction chemistry allows for resulting materials to exhibit specificity. Based on the most favorable materials, which included metal-oxides and metal-organic frameworks, impedance measurements and devices were pursued as the plasmonic resonance of these materials were far too weak to make sensible measurements or device architectures. Our results show that there are materials electronically sensitive enough to enable impedimetric

15. SUBJECT TERMS
Impedance Spectroscopy, Toxic and Explosive Chemicals, Fe2O3, zirconium hydroxide, nanoparticles

16. SECURITY CLASSIFICATION OF:			17. LIMITATION OF ABSTRACT	15. NUMBER OF PAGES	19a. NAME OF RESPONSIBLE PERSON
a. REPORT	b. ABSTRACT	c. THIS PAGE			S Allen
UU	UU	UU	UU		19b. TELEPHONE NUMBER: 805-893-7134

Report Title

Final Report: Dielectric Sensing of Toxic and Explosive Chemicals via Impedance Spectroscopy and Plasmonic Resonance (research area 11: STIR)

ABSTRACT

The primary focus of this nine-month effort was to develop electronic sensors for hazardous chemicals. The first step was to identify material(s) that have interaction potential with chemicals of interest. In particular, specific reaction chemistry allows for resulting materials to exhibit specificity. Based on the most favorable materials, which included metal-oxides and metal-organic frameworks, impedance measurements and devices were pursued as the plasmonic resonance of these materials were far too weak to make sensible measurements or device architectures. Our results show that there are materials electronically sensitive enough to enable impedimetric devices that use the frequency-dependence "fingerprint" of AC impedance to improve selectivity.

Enter List of papers submitted or published that acknowledge ARO support from the start of the project to the date of this printing. List the papers, including journal references, in the following categories:

(a) Papers published in peer-reviewed journals (N/A for none)

Received Paper

TOTAL:

Number of Papers published in peer-reviewed journals:

(b) Papers published in non-peer-reviewed journals (N/A for none)

Received Paper

TOTAL:

Number of Papers published in non peer-reviewed journals:

(c) Presentations

1) Coleman Harris, Jennifer Soliz, Andrew Klevitch, Joseph Rossin, Augustus Fountain III, Gregory Peterson, and Adam Hauser, "Sensing of NO2 with Zirconium Hydroxide via Electrical Impedance Spectroscopy," 2016 American Physical Society March Meeting, Baltimore, MD.

2) Joshua J. Phillips, Jennifer R. Soliz, and Adam J. Hauser, "XMCD and Impedance Analysis of Fe2O3 Nanoparticles for Explosive and Chemical Warfare Agent Sensing Applications," 2016 American Physical Society March Meeting, Baltimore, MD.

Number of Presentations: 0.00

Non Peer-Reviewed Conference Proceeding publications (other than abstracts):

Received Paper

TOTAL:

Number of Non Peer-Reviewed Conference Proceeding publications (other than abstracts):

Peer-Reviewed Conference Proceeding publications (other than abstracts):

Received Paper

TOTAL:

Number of Peer-Reviewed Conference Proceeding publications (other than abstracts):

(d) Manuscripts

Received Paper

TOTAL:

Number of Manuscripts:

Books

Received Book

TOTAL:

Received	Book Chapter

TOTAL:

Patents Submitted

Patents Awarded

Awards

Graduate Students

NAME	PERCENT_SUPPORTED
FTE Equivalent:	
Total Number:	

Names of Post Doctorates

NAME	PERCENT_SUPPORTED
FTE Equivalent:	
Total Number:	

Names of Faculty Supported

NAME	PERCENT_SUPPORTED
FTE Equivalent:	
Total Number:	

Names of Under Graduate students supported

NAME	PERCENT_SUPPORTED	Discipline
Coleman Harris	0.10	Computer Science
Joshua Phillips	0.10	Mathematics
Andrew Klevitch	0.10	Physics
FTE Equivalent:	**0.30**	
Total Number:	**3**	

Student Metrics

This section only applies to graduating undergraduates supported by this agreement in this reporting period

The number of undergraduates funded by this agreement who graduated during this period: 0.00

The number of undergraduates funded by this agreement who graduated during this period with a degree in science, mathematics, engineering, or technology fields:..... 0.00

The number of undergraduates funded by your agreement who graduated during this period and will continue to pursue a graduate or Ph.D. degree in science, mathematics, engineering, or technology fields:..... 0.00

Number of graduating undergraduates who achieved a 3.5 GPA to 4.0 (4.0 max scale):..... 0.00

Number of graduating undergraduates funded by a DoD funded Center of Excellence grant for Education, Research and Engineering:..... 0.00

The number of undergraduates funded by your agreement who graduated during this period and intend to work for the Department of Defense 0.00

The number of undergraduates funded by your agreement who graduated during this period and will receive scholarships or fellowships for further studies in science, mathematics, engineering or technology fields: 0.00

Names of Personnel receiving masters degrees

NAME

Total Number:

Names of personnel receiving PHDs

NAME

Total Number:

Names of other research staff

NAME	PERCENT_SUPPORTED

FTE Equivalent:

Total Number:

Sub Contractors (DD882)

Inventions (DD882)

Scientific Progress

Technology Transfer

ARO STIR FINAL PROGRESS REPORT, GRANT NUMBER W911NF-15-1-0104

"Dielectric Sensing of Toxic and Explosive Chemicals via Impedance Spectroscopy and Plasmonic Resonance"

Dr. S. James Allen, Department of Physics, University of California, Santa Barbara
Dr. Adam J. Hauser, Department of Physics, University of Alabama, Tuscaloosa

STATEMENT OF THE PROBLEM STUDIED

Current deployable explosives and toxic chemical sensing methods utilize ion mobility mass spectrometry, gas chromatograph mass spectrometry, X-ray imaging, Raman spectroscopy, and other such techniques. While these techniques are highly selective, each method has its own shortcomings, such as low resolution, competing ion or molecule side reactions, response variation from different compositions of analytes, limited response range, and time-consumption.[1] In addition, most of these techniques are bulky and require significant training for proper utilization. For example, as of 2011, the state-of-the-art for organophosphates was the Department of Defense HAPSITE (Hazardous Air Pollutants on Site) system, a 70-pound "portable" gas chromatograph mass spectrometer that costs well over $100,000 per unit, not including the costs of weekly maintenance and a field team of specially trained personnel[2].

Worse yet, although the most rapid detection method at the time, HAPSITE fails the requirements for rapid detection in emergency situations, with a 30 minute exposure required for detection of levels in which a 10-minute exposure will have debilitating effects in a significant fraction of the population. Although fine for a military advance team, this sensor is not adequate for defense applications, and certainly not cheap or sensitive enough for civilian applications such as prevention of OP exposure at home or in the workplace due to pesticides or other aforementioned sources. A potential approach to sense explosives and other toxic chemicals while circumventing the aforementioned shortcomings is to target materials that exhibit changes in the dielectric constant upon chemical exposure. Because the dielectric constant of a material can be tuned to specific interactions, this approach offers potential specificity. Integrating dielectrics into chemical sensors is desirable as they can offer portability, tunability, simplicity, low costs, and rapid response times.

The primary focus of this nine-month effort was to develop electronic sensors for hazardous chemicals. The first step was to identify material(s) that have interaction potential with chemicals of interest. In particular, specific reaction chemistry allows for resulting materials to exhibit specificity. Based on the most favorable materials, which included metal-oxides and metal-organic frameworks, impedance measurements and devices were pursued as the plasmonic resonance of these materials were far too weak to make sensible measurements or device architectures. Our results show that there are materials electronically sensitive enough to enable impedimetric devices that use the frequency-dependence "fingerprint" of AC impedance to improve selectivity.

SUMMARY OF THE MOST IMPORTANT RESULTS

Fe_2O_3 nanoparticles. Iron-based compounds have been shown to rapidly degrade CWA structural analogs on contact[3-5]. Iron-based oxides are considered favorable not only for rapid reaction time, but are both cheap and environmentally friendly. In collaboration with Dr. Jennifer Soliz at Edgewood Chemical Biological Center, we identified Fe_2O_3 as a promising candidate for OP detection, using CWA structural analogs such as dimethyl methylphosphonate (DMMP) and dimethyl chlorophosphate (DMCP)[5]. As compared to the adsorption pathway of many oxides, Fe_2O_3 has been shown to undergo a strong binding to OP compounds[6-10]. The stoichiometric reaction mechanism, an irreversible process, is shown in **Figure 1** for CWA structural analogs (a) dimethyl methylphosphonate (DMMP) and (b) diemthyl chlorophosphonate (DMCP). The analogs are shown to initially bond through the phosphoryl (P=O) oxygen atom on the Fe-sites, creating a bridging phosphoryl species. Through this reaction, Fe^{3+} undergoes reduction in cation valency to Fe^{2+}; thereby causing a valence change on the nanoparticle surface and molecular dissociation of the OP compounds.

Our collaboration has for the first time studied the effects of various compounds on the magnetic and electronic states of the system, with an eye toward adequate sensitivity and selectivity. By converting Fe^{3+} to Fe^{2+} upon contact, OPs convert the magnetic Fe_2O_3 to FeO and cause both a change in magnetic moment and some change in electrical resistivity. We see the drop in magnetic moment determined by both bulk magnetometry and x-ray magnetic

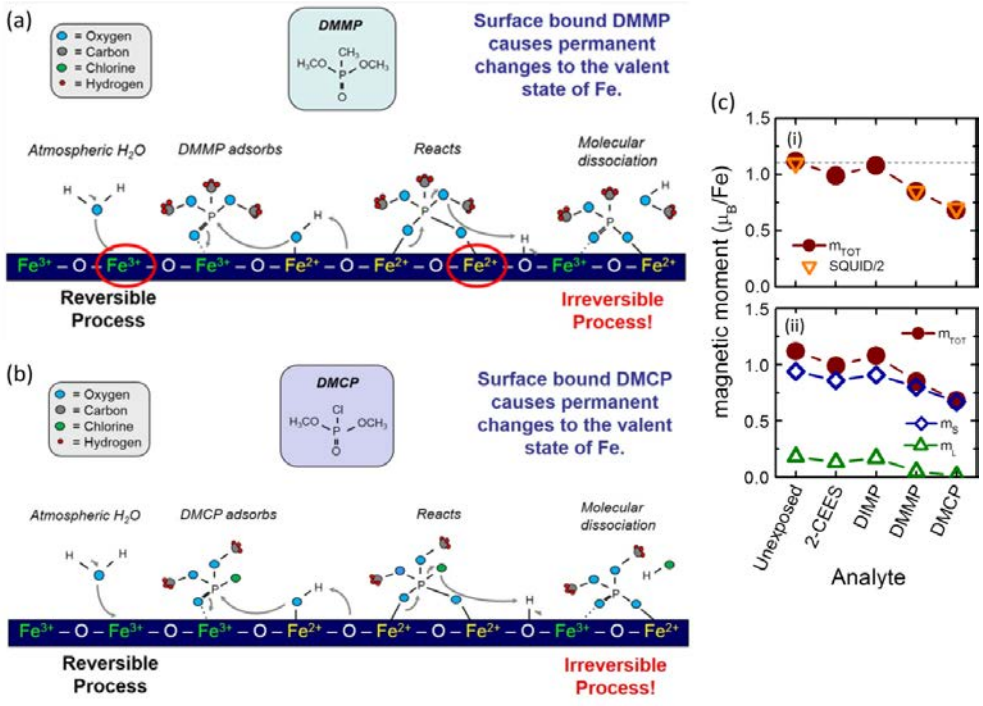

Figure 1. Schematic of the adsorption and molecular dissociation of (a) *dimethyl methylphosphonate* (DMMP) and (b) *dimethyl chlorophosphonate* (DMCP) with Fe_2O_3. (c) Fe-site magnetic moment in Fe_2O_3 by XMCD after 10% volume per gram saturated exposures of explosive (2-CEES) and G-agent (DIMP, DMMP, DMCP) analogs. (i) Total moment/Fe site by XMCD (solid red circles), as compared to macroscopic measurements by SQUID (orange triangles). (ii) Breakdown of the total moment (red circles) into both spin (blue diamonds) and orbital (green triangles) components.

circular dichroism measurements at beamline 4-ID-C at Argonne National Laboratory's Advanced Photon Source in **Figure 1 (c)**, wherein a 10% volume per gram saturated exposure of DMCP to a pressed pellet of 30% α-phase/70% γ-phase Fe_2O_3 yields nearly a 50% drop in moment. X-ray absorption spectroscopy analysis confirms our mechanism, as DMCP-exposed nanoparticles show large changes in both Fe and O spectra commensurate with the transition to Fe^{2+} states. It is worth noting that exposure to the lesser toxic sulfur mustard agent analog, *2*-chloroethyl ethyl sulfide (2-CEES), resulted in a small decrease in magnetic moment. However, the comparatively large change in moment upon exposure to some (but not all) G-agent compounds, put together with the unique reaction Fe_2O_3 undergoes with OPs imply that Fe_2O_3 sensors may result in specificity to one or a small number of organophosphates.

However, magnetic sensors cannot be made as small, robust, and cheaply as electrical sensors designed around a change in impedance/resistance upon exposure. **Figure 2** shows the percent change in (a) impedance Z and (b) resistance R (the real component of Z) as a function of frequency, for pressed pellet capacitor geometry when exposed to the two OP compounds (DMMP and DMCP) that showed magnetic evidence for chemical reaction. Our impedance work was done using pressed pellets of commercially available 23 nm diameter nanoparticles with maximum surface areas of 30-60 m^2/g. This number is likely reduced practically due to the bulk-like state of the pellet. In practice, devices can be made using impedance or resistance. We observe large on/off ratios in impedance (150%) and resistivity (480%) in the 100 kHz – 1 MHz range, an easily attained frequency. Shifts are also large as one approaches the DC limit, indicating that DC device application is also a strong possibility.

It is exceedingly useful that even within the organophosphate subclass the two compounds shown show shifts in different directions. This would allow any device to distinguish between different species quickly, and speaks to another useful application of the proposed impedance devices; impedance fingerprinting, wherein the frequency profile (or simply several points therein) create a unique "shift fingerprint" with which high specificity can be determined in very short order. In addition, Fe_2O_3 nanoparticles have recently shown smaller (~17%) sensitivity to NO_2 gas, helping the case for Fe_2O_3's OP selectivity[11].

We point out that a small barrier to future devices exists in that the same irreversible chemical process that makes Fe_2O_3 nanoparticles reactive with high change in impedance also makes restricts the number of uses one may use it for. For instance, while the material would make an excellent detector or dosimeter, a device would be a one-time use product if left with only measurement capability (although this is true of nearly every sensor). The low cost of the device mitigates the downside of such a trait, especially as we bring the device size down to that of a credit card, or for wearables, a small patch. Additionally, it is possible that purging of the adsorbate

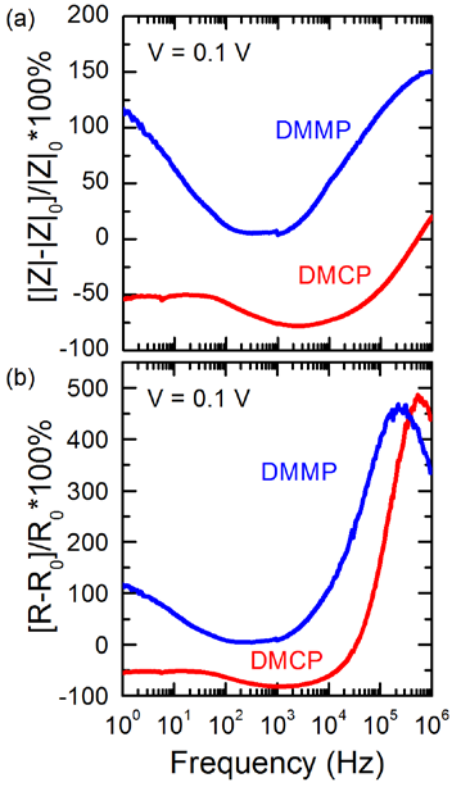

Figure 2. Percent changes in (a) impedance and (b) resistance as a function of frequency in pressed pellets of 23 nm diameter Fe_2O_3 nanoparticles from DMMP (blue) and DMCP (red) exposures.

and reversal of the Fe_2O_3 → FeO reaction could implemented by reaction with oxygen gas, perhaps ozone treatment or gentle heating in air[10]. Further study, especially within the thermal and chemical constraints of other device components, will be necessary to determine the range of device utility and reusability.

Porous $Zr(OH)_4$ particles. Zirconium hydroxide is another cheap, commercially available material of interest due to high decontamination performance on an assortment of dangerous chemicals[12-17]. Peterson (ECBC) and co-workers have found that the exceptional reactivity is due to the presence of both bridging and terminal hydroxyl groups, allowing both acids and bases to react with the material, while performing in both dry and humid conditions. $Zr(OH)_4$'s primary advantage over other metal oxides is its many built-in hydroxyl groups, as it does not require the previous adsorption of an –OH group to enable hydrolysis. Additionally, particles of zirconium hydroxide exhibit local regions of crystallinity amongst the amorphous matrix, resulting in a highly porous material and resultant high surface-to-volume area even when the particles are on the microscale: In the materials work we will show, we used 15 μm $Zr(OH)_4$ particles with surface area 406 m^2/g and pore volume 0.81 cc/g. The surface area in this case, despite particles three orders of magnitude bigger than the aforementioned Fe_2O_3 nanoparticles, has a surface to volume ratio an order of magnitude higher.

The choice of $Zr(OH)_4$ for organophosphate detection is made straightforward by the work of Bandosz *et al*, who thoroughly characterized the rapid decontamination of chemical warfare agents VX, soman (GD) and distilled mustard gas (HD)[18]. The work shows that $Zr(OH)_4$ has an incredibly fast detoxification timescale for VX (1 min), while GD (8.7 min) and HD (2.3 hr) detoxify more slowly.

We note that the shift fingerprint was seen in the Fe_2O_3 impedance data earlier (**Figure 2**), despite any clear difference in reaction pathways. In $Zr(OH)_4$, even more distinctive features occur.

During this funding term, $Zr(OH)_4$ impedance reactivity to NO_2 has been measured. Pervious work by Singh *et al* has shown by photoluminescence and electron microscopy that the observed reactivity stems from replacement of hydroxyl groups with chemisorbed NO_3[17]. In our work, 13 mm diameter pressed pellets were exposed to a range of NO_2 dosages from 0 to 1000 ppm·hr, and characterized by AC Impedance Analysis with a constant voltage of 0.1 V. The magnitude |Z| and phase angle θ of the impedance measured as a function of frequency is shown in **Figures 3a and 3b,** respectively, for NO_2 exposures of 0, 50, 200, and 1,000 ppm·hr. An applied voltage of 0.1V was used for all data points. We observe changes in |Z| over many orders of magnitude, indicating a strong

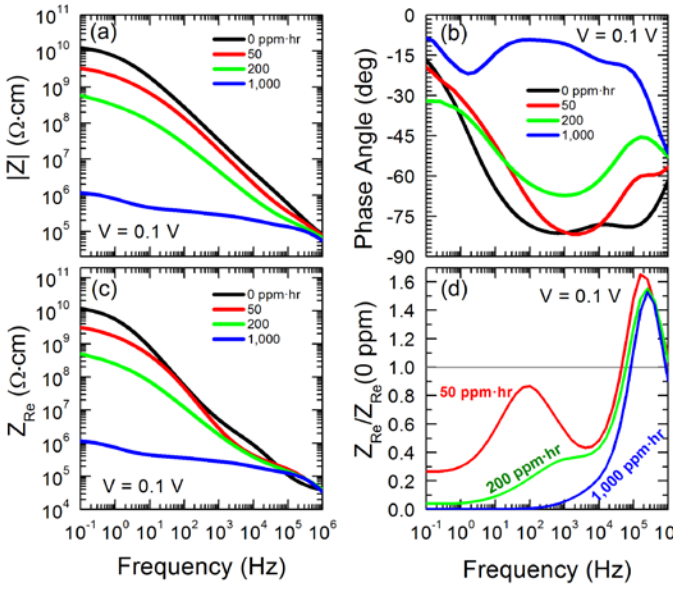

Figure 3. (a) Magnitude |Z|, (b) phase angle θ, (c) real component Z_{Re} of the impedance as a function of frequency. (d) $Z_{Re}/Z_{Re}(0)$ for various NO_2 exposure dosages, where $Z_{Re}(0)$ is the real component of impedance for unexposed $Zr(OH)_4$.

sensitivity to NO_2. We also observe a general trend in phase angle from -90° towards 0°, suggesting a trend from capacitive to resistive behavior, likely a reflection of chemical changes creating conductive pathways in the pellet. By a dosage level of 1,000 ppm·hr the phase angle is approaching zero at nearly all frequencies, and a series of three "bumps" can be seen above the DC limit; a pair centered around 10 and 100 Hz, and a higher frequency feature near 100 kHz that can be seen for even low exposure levels. While these features are broad and not easily analyzed, they inform the equivalent circuit to be used later in the paper for fitting and analysis.

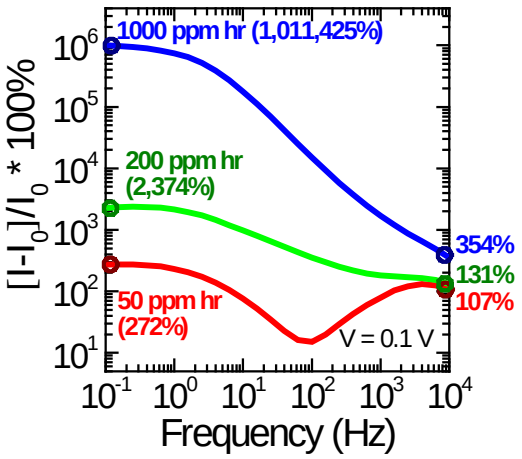

Figure 4. Percent changes in current for a $Zr(OH)_4$ parallel capacitor device with applied voltage V = 0.1 V, for total NO_2 dosages of 50 (red), 200 (green) and 1000 (blue) ppm·hr. Percentages in parenthesis are the percent increase in device current at 0.1 Hz, close to the DC limit. Values at 10 kHz are displayed on the right edge.

If one imagines our pellet/electrode setup as a simple resistive NO_2 detection device in line with a 0.1 V AC source, the easiest signal extraction method would be measurement of the resultant current magnitude. This is dictated by the resistance R, defined as the real component of the impedance, $Z_{Re} = |Z| \cos \theta$. We plot Z_{Re} as a function of frequency in **Figure 3c**. Note that as dosage is increased, we see less and less difference between Z_{Re} and $|Z|$ as the system approaches pure resistive transport. We display the changes in Z_{Re} upon exposure as compared to the initial, unexposed state in **Figure 3d**. One sees large drops in resistance below 10 kHz even down to the lowest dosage level of 50 ppm·hr . We again see features at approximately 100 Hz and 100 kHz, reflecting the contribution of the phase angle to Z_{Re}.

The percent change in signal current due to NO_2 exposure is shown in log scale in **Figure 4**, up to 10 kHz. The peak values for signal change all occur below 1 Hz, near the DC limit. For 50, 200, and 1,000 ppm·hr dosages, we see signal changes of 272%, 2,374%, and 1,011,425%, respectively. These values are proof of high sensitivity and wide dosage range, indicating that $Zr(OH)_4$, if found to be selective, may be an excellent choice for future use in NO_2 detectors or dosimeters. Although the $Zr(OH)_4$ grains are very porous, we note that the pellet was exposed after pressing, suggesting that further sensitivity gains may be possible by optimizing the surface-to-volume ratio of the material upon exposure.

The results of Figure 4 show zirconium hydroxide to have high sensitivity across a large dosage range that extends through the lethal concentration 50 dosage of 360 ppm·hr. The range suggests zirconium hydroxide as an excellent dosimeter for its large cumulative range, and also as a static point detector/monitor, wherein the change in current can be cross-checked with a frequency-dependent calibration curve to obtain the real-time NO_2 concentration. Additionally, the significant impedance shift seen even at 50 ppm·hr strongly suggests sensitivity can be achieved down to the point where pulmonary function begins to be affected (2-3 ppm). This functionality is especially likely considering that a pressed pellet was exposed as opposed to loose powder or the thin film structure proposed herein.

Complex Impedance Analysis was done with the fitting program ZView (Scribner Associates, Inc)[19]. A variety of equivalent circuit models that have been used previously were attempted[20-27]. We find fitting to be achieved with an arrangement as shown in **Figure 5a**, utilizing three resistor-constant phase element (CPE[28]) pairs in series[29-31]. This arrangement is motivated by phase angle features in **Figure 3b**, as well as the tell-tale semicircular features in the Nyquist plot (discussed below) that are best modeled with R-CPE pairs. We did not find a similar quality fit across the entire range for any other equivalent circuit. Due to the high impedance of the materials, the series resistor in the circuit to simulate lead resistance has negligible value and the same element values and fit quality are extracted with or without its presence. Finally, we attempted to change the order and starting parameters of each fit to check for local minima or multiple solutions, but all good fits resulted in similar results.

Figure 5b shows a log-log plot of the imaginary (Z" = |Z| sin θ) component of the impedance as a function of the real component Z', a so-called Nyquist Plot. Data points are displayed as scatter points, with our equivalent circuit fits shown as black lines behind the point. From the fits, we can extract resistance and capacitance values for each component in Figure 4a, and then determine the dielectric relaxation frequency 1/RC, as plotted for our three as-yet unassigned elements in **Figure 6a**. Our fits find three general frequency ranges, one near 5-20 Hz, one near 50-250 Hz, and another in the 20-200 KHz range. Immediately, one sees an anomaly in frequency 1 of the 1,000 ppm·hr, several orders above the rest.

We approach assignment of frequencies by the typical approach of assigning the highest frequency (1) to the grain interior, the next-highest (2) to grain boundary effects, and the lowest (3) to ionic diffusion effects[23,25,32]. In the case of porous grains such as $Zr(OH)_4$, we posit that the bulk-like grain interior component will remain fairly constant in resistance as ever greater portions are changed by chemical reaction, and the capacitance will also remain constant for a time. As the core becomes extremely small and/or disappears, the capacitance will collapse as it is shorted by defects or alternate pathways, resulting in unphysical results. As the chemically changed outer portion of each grain increases in size, each adsorption site will become increasingly interconnected with other grains and show marked decreases in resistivity as the changed "shell" increases in size within in grain. Meanwhile, the ionic buildup due to adsorption will create a measurable "double-layer capacitance" across grain

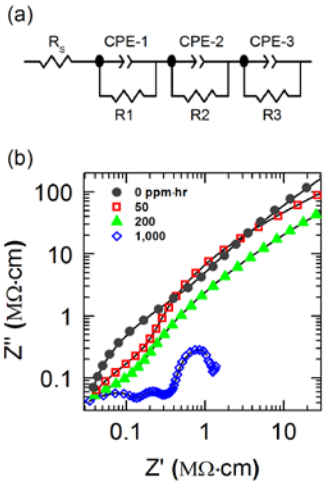

Figure 5. (a) Equivalent circuit schematic used for AC impedance analysis. R_S: series/lead resistance. CPE: constant phase element. (b) Log-log Nyquist plot (symbols) and equivalent circuit fits (lines) for $Zr(OH)_4$ pellets subjected0 to NO_2 doses of 0 (grey solid circle), 50 (red open square), 200 (green solid triangle), and 1000 (blue open diamond) ppm·hr.

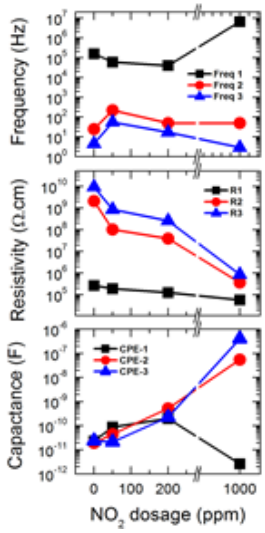

Figure 6. (a) Dielectric relaxation frequencies (= 1/RC) of each of the three resistor/constant phase element pairs, as fit to our data using the equivalent circuit in Figure 4(a). (b) Resistivity and (c) capacitance fit values for the resistor and constant phase element (respectively) corresponding to each R-CPE pair.

boundaries that will increase as the ionically charged portion increases in thickness. We thus arrive at a physical picture wherein the grain boundary and ionic processes are both within the chemically altered regions and their impedance properties are strongly tied together

SUMMARY

This STIR project has determined that frequency-dependent impedance devices are the most likely pathway to sensitive and selective devices for toxic and explosive chemicals. The identified materials of choice have negligible localized surface plasmonic resonance and show only marginal magnetic sensitivity to exposure with no clear pathway for selectivity. However, by using the frequency-dependent impedance/resistance shifts, we believe that a pathway to chemical fingerprinting exists and represents a major opportunity going forward in chemical sensing. Going forward, impedance devices with high-surface area to volume ratios must be pursued to determine if the impedimetric sensitivities seen in this project can be replicated and improved upon.

BIBLIOGRAPHY

[1] H. H.; Simpson Hill, G.," Capabilities and limitations of ion mobility spectrometry for field screening applications." Field Anal. Chem. Tech. **1**, 119 (1997).

[2] Mark N Goltz, Dong S Kim, and LeeAnn Racz,"Using Nanotechnology to Detect Nerve Agents" AIR UNIV MAXWELL AFB AL AIR FORCE RESEARCH INST (2011).

[3] Radek Zboril, Marek Andrle, Frantisek Oplustil, Libor Machala, Jiri Tucek, Jan Filip, Zdenek Marusak, and Virender K Sharma,"Treatment of chemical warfare agents by zero-valent iron nanoparticles and ferrate (VI)/(III) composite" Journal of hazardous materials **211**, 126 (2012).

[4] Václav Štengl, Jiří Henych, Pavel Janoš, and Miroslav Skoumal, in *Reviews of Environmental Contamination and Toxicology Volume 236* (Springer, 2016), pp. 239.

[5] Christopher J. Karwacki Jennifer R. Soliz, Wesley O. Gordon, Alex Balboa, John J. Mahle, Adam J. Hauser, Konrad M. Bussmann, Michael S. Osofsky, Brendan G. DeLacy, and Zachary Zander "A Fundamental Understanding of the Structural and Magnetic Properties Impacted From the Molecular Dissociation of Chemical Warfare Agents Using Fe2O3 Nanoparticles" In Preparation.

[6] V. N. Sheinker Mark B. Mitchell, and Eric A. Mintz,"Adsorption and decomposition of dimethyl methylphosphonate on metal oxides" Journal of Physical Chemistry B **101** (51), 11192 (1997).

[7] Michael A. Henderson,"Surface Chemistry of Trimethyl Phosphate on α-Fe2O3" The Journal of Physical Chemistry C **115** (47), 23527 (2011).

[8] M. A. Henderson, T. Jin, and J. M. White,"A TPD/AES study of the interaction of dimethyl methylphosphonate with iron oxide (.alpha.-Fe2O3) and silicon dioxide" The Journal of Physical Chemistry **90** (19), 4607 (1986).

[9] Viktor N. Sheinker and Mark B. Mitchell,"Quantitative Study of the Decomposition of Dimethyl Methylphosphonate (DMMP) on Metal Oxides at Room Temperature and Above" Chemistry of Materials **14** (3), 1257 (2002).

[10] Teweldemedhin M. Tesfai, V. N. Sheinker, and Mark B. Mitchell,"Decomposition of Dimethyl Methylphosphonate (DMMP) on Alumina-Supported Iron Oxide" The Journal of Physical Chemistry B **102** (38), 7299 (1998).

[11] S. T. Navale, D. K. Bandgar, S. R. Nalage, G. D. Khuspe, M. A. Chougule, Y. D. Kolekar, Shashwati Sen, and V. B. Patil,"Synthesis of Fe2O3 nanoparticles for nitrogen dioxide gas sensing applications" Ceramics International **39** (6), 6453 (2013).

[12] T Grant Glover, Gregory W Peterson, Jared B DeCoste, and Matthew A Browe,"Adsorption of ammonia by sulfuric acid treated zirconium hydroxide" Langmuir **28** (28), 10478 (2012).

[13] Gregory W Peterson, Christopher J Karwacki, William B Feaver, and Joseph A Rossin,"Zirconium hydroxide as a reactive substrate for the removal of sulfur dioxide" Industrial & Engineering Chemistry Research **48** (4), 1694 (2009).

[14] Gregory W Peterson, Joseph A Rossin, Christopher J Karwacki, and T Grant Glover,"Surface chemistry and morphology of zirconia polymorphs and the influence on sulfur dioxide removal" The Journal of Physical Chemistry C **115** (19), 9644 (2011).

[15] Gregory W Peterson and Joseph A Rossin,"Removal of chlorine gases from streams of air using reactive zirconium hydroxide based filtration media" Industrial & Engineering Chemistry Research **51** (6), 2675 (2012).

[16] Gregory W. Peterson, Joseph A. Rossin, Jared B. DeCoste, Kato L. Killops, Matthew Browe, Erica Valdes, and Paulette Jones,"Zirconium Hydroxide–Metal–Organic Framework Composites for Toxic Chemical Removal" Industrial & Engineering Chemistry Research **52** (15), 5462 (2013).

[17] Jagdeep Singh, Anupama Mukherjee, Sandip K Sengupta, Jisun Im, Gregory W Peterson, and James E Whitten,"Sulfur dioxide and nitrogen dioxide adsorption on zinc oxide and zirconium hydroxide nanoparticles and the effect on photoluminescence" Applied Surface Science **258** (15), 5778 (2012).

[18] Teresa J. Bandosz, Matt Laskoski, John Mahle, Gregory Mogilevsky, Gregory W. Peterson, Joseph a Rossin, and George W. Wagner,"Reactions of VX, GD, and HD with Zr(OH)4: Near instantaneous decontamination of VX" Journal of Physical Chemistry C **116**, 11606 (2012).

[19] D Johnson,"Zview version 2.9 b" Scribner Associates: Southern Pines, NC, USA (2004).

[20] O. S. Doroshkevych, A. V. Shylo, O. V. Saprukina, I. A. Danilenko, T. E. Konstantinova, and L. A. Ahkozov,"Impedance Spectroscopy of Concentrated Zirconia Nanopowder Dispersed Systems Experimental Technique" World Journal of Condensed Matter Physics **Vol.02No.01**, 4 (2012).

[21] J. Lee, J. H. Hwang, J. J. Mashek, T. O. Mason, A. E. Miller, and R. W. Siegel,"Impedance spectroscopy of grain boundaries in nanophase ZnO" Journal of Materials Research **10** (09), 2295 (1995).

[22] Suman Pokhrel, C. E. Simion, V. Quemener, N. Bârsan, and U. Weimar,"Investigations of conduction mechanism in Cr2O3 gas sensing thick films by ac impedance spectroscopy and work function changes measurements" Sensors and Actuators B: Chemical **133** (1), 78 (2008).

[23] Bibhutibhushan Show, Nillohit Mukherjee, and Anup Mondal,"Electrochemically synthesized microcrystalline tin sulphide thin films: high dielectric stability with lower relaxation time and efficient photochemical and photoelectrochemical properties" RSC Advances **4** (102), 58740 (2014).

[24] R Gerhardt and AS Nowick,"Grain-Boundary Effect in Ceria Doped with Trivalent Cations: I, Electrical Measurements" Journal of the American Ceramic Society **69** (9), 641 (1986).

[25] R. Gerhardt,"Impedance and dielectric spectroscopy revisited: Distinguishing localized relaxation from long-range conductivity" Journal of Physics and Chemistry of Solids **55** (12), 1491 (1994).

[26] Jun Hyuk Yang, Chung Wung Bark, Kyung Hwan Kim, and Hyung Wook Choi,"Characteristics of the Dye-Sensitized Solar Cells Using TiO2 Nanotubes Treated with TiCl4" Materials **7** (5), 3522 (2014).

[27] J Ross Macdonald and E Barsoukov,"Impedance spectroscopy: theory, experiment, and applications" History **1**, 8 (2005).

[28] GJ Brug, ALG Van Den Eeden, M Sluyters-Rehbach, and JH Sluyters,"The analysis of electrode impedances complicated by the presence of a constant phase element" Journal of electroanalytical chemistry and interfacial electrochemistry **176** (1), 275 (1984).
[29] Nikolaos Bonanos, Peter Holtappels, and MJ Jørgensen, presented at the 5th European Solid Oxide Fuel Cell Forum, 2002 (unpublished).
[30] Xiaoqing Zhang, Yihua Zhu, Xiaoling Yang, Siwen Wang, Jianhua Shen, Babao Lin, and Chunzhong Li,"Enhanced visible light photocatalytic activity of interlayer-isolated triplex Ag@SiO2@TiO2 core-shell nanoparticles." Nanoscale **5**, 3359 (2013).
[31] Hugo Fricke,"The Maxwell-Wagner dispersion in a suspension of ellipsoids" The Journal of Physical Chemistry **57** (9), 934 (1953).
[32] Da Yu Wang and A. S. Nowick,"The “grain-boundary effect” in doped ceria solid electrolytes" Journal of Solid State Chemistry **35** (3), 325 (1980).